

Fast n -point correlation functions and three-point lensing application

Lucy Liuxuan Zhang^{a,b} Ue-Li Pen^{a,c}

^a*Canadian Institute for Theoretical Astrophysics,
University of Toronto, M5S 3H8, Canada*

^b*lxzhang@cita.utoronto.ca*

^c*pen@cita.utoronto.ca*

Abstract

We present a new algorithm to rapidly compute the two-point (2PCF), three-point (3PCF) and n -point (n -PCF) correlation functions in roughly $O(N \log N)$ time for N particles, instead of $O(N^n)$ as required by brute force approaches. The algorithm enables an estimate of the full 3PCF for as many as 10^6 galaxies. This technique exploits node-to-node correlations of a recursive bisectional binary tree. A balanced tree construction minimizes the depth of the tree and the worst case error at each node. The algorithm presented in this paper can be applied to problems with arbitrary geometry.

We describe the detailed implementation to compute the two point function and all eight components of the 3PCF for a two-component field, with attention to shear fields generated by gravitational lensing. We also generalize the algorithm to compute the n -point correlation function for a scalar field in k dimensions where n and k are arbitrary positive integers.

Key words: statistics – large-scale structure – gravitational lensing.

PACS: 98.62.Sb

1 Introduction

The correlation functions are important tools for computation and analysis in many areas of astrophysics. They are introduced into modern cosmology by people such as Totsuji and Kihara (1969) and Peebles (1973). Some prominent applications of the correlation functions can be found in areas such as galaxy clustering, CMB, and weak lensing. For a scalar field $\rho(\mathbf{X})$, the two-point correlation function (2PCF) ξ_2 and the three-point correlation function (3PCF)

ξ_3 are defined as

$$\xi_2(s) = \langle \rho(\mathbf{X}_1)\rho(\mathbf{X}_2) \rangle \quad (1)$$

and

$$\xi_3(s_1, s_2, s_3) = \langle \rho(\mathbf{X}_1)\rho(\mathbf{X}_2)\rho(\mathbf{X}_3) \rangle \quad (2)$$

where s is the distance between \mathbf{X}_1 and \mathbf{X}_2 , and s_i represents the distance between \mathbf{X}_j and \mathbf{X}_k with $i \neq j \neq k$.

The n -point correlation function (n -PCF) of a scalar field $\rho(\mathbf{X})$ is a function of all the possible arrangements of n points chosen from the system. As a function of configurations, the value of the n -point function is the expectation value of the product of the field quantity ρ , sampled at a set of n points conforming to a specific configuration. The one-point correlation function (1PCF) is simply the weighted average of ρ over all data points; in the case of the 2PCF, the spacial configuration is characterized by the separation between two points. From the definition of the ensemble average, the n -point correlation function for a system of N points can be computed by looping through all combinations of n points, determining the configuration category for each combination, and accumulating necessary statistics, such as the sum of products of the weighted ρ 's and that of the weights, under the appropriate configuration category. Outside of the loop, we divide the sum of the products of the weighted ρ 's by the sum of the products of their weights for each configuration to obtain the expectation value of the product of ρ 's at any n points as a function of configurations. This brute force approach amounts to a loop through $N(N - 1)\dots(N - n + 1)$ combinations, which is intrinsically an $O(N^n)$ computation. For N of astronomical interest, such significant cost makes it impossible to compute by brute force the full correlation function of order n greater than two.

In fact, even for $n=2$, more efficient algorithms are often necessary and have been developed. Early applications (Wittman et al., 2000) of the two point function in weak gravitational lensing summed pairs, which is an $O(N^2)$ algorithm. Since an auto-correlation is a convolution, several procedures exist to reduce it to $O(N \log N)$ using either the well-known fast Fourier transforms or a tree summation (Barnes and Hut, 1986). See Pen et al. (2003) for an example of a 2PCF algorithm in 2D using FFT. In the astrophysical literature, algorithms to compute correlations of arbitrary order have been presented by Moore et al. (2001). These are reported to scale as $O(N^{3/2})$ for the 2PCF computation.

Recent progress has been made in effort to speed up the computation of the three-point correlation function. After this work was completed, we became

aware of an independent implementation of a very similar algorithm for the 3PCF by Jarvis et al. (2003) based on an $O(N \log N)$ implementation of the Moore et al. (2001) algorithm. Recently, an unpublished $O(N)$ algorithm for computing the n -point correlation function is also reported to exist (Gray et al., 2004). All of these algorithms are based on the idea of kd-trees which is first proposed by (Bentley, 1975).

In this paper, we will describe a new, general and fast algorithm for the n -PCF computation in arbitrary dimensions, with focus on the implementation of correlation functions in 2D weak lensing data analyses. As mentioned in Schneider and Lombardi (2003), the two-point correlation function has been a popular method to analyze lensing data because it can be easily observed and cheaply computed; in addition, all second-order statistical measures can be derived in terms of the two-point function. On the other hand, Pen et al. (2003) used the three-point correlation function to measure the skewness of the shear which helps break the $\Omega - \sigma_8$ degeneracy. As expected, the 3PCF is computationally much more complex and expensive. Most detections of the 3PCF or higher moments merely take into account sparse subsets of the possible configurations, such as the equilateral triangles (Santos et al., 2002). Even the computation of a partial 3PCF required the use of a supercomputer (Sandvik and Magueijo, 2001). The challenge of computing the *full* 3PCF is also illustrated by Verde et al. (2002), who used only two different triangle configurations to estimate the bispectrum, significantly reducing the number of triangles from $75\,792^3 \sim 4 \times 10^{14}$ to 80×10^6 . Eriksen et al. (2003) estimated the n -PCF in $O(N^n)$ time with a small prefactor for Monte Carlo analysis. They also pointed out that higher order n -point correlation functions are notorious for being computationally expensive. Besides its speed, our tree method of computing the 3PCF is advantageous to the fourier space computation in that it is free of geometric restrictions. The tree structure allows easy extension to computing correlation functions of arbitrary order in higher dimensional space.

Fortunately, the new algorithm developed here makes it tractable to handle rapidly increasing cosmological data sets. Now using a single-processor machine, we are able to compute the full shear 3PCF for 10^6 galaxies. Besides its speed, it is superior to the existing 3PCF FFT algorithm (Pen et al., 2003) in its freedom from geometric restrictions.

This paper consists of six sections. In section 2, we describe in detail the construction of the recursive bisectional binary tree which is the basis for rapid computation of the n -PCF. In section 3, we show how to compute the 2PCF using the tree by first discussing the process of 'subdivision' and its dependence on the 'critical open angle'¹, then reviewing the accumulation of two-point statistics and, for a spin-2 field, our choice of coordinates for

¹ The term 'open angle' is coined by Barnes and Hut (1986).

a given pair of nodes. In section 4, we conveniently extend the method for computing the 2PCF to accommodate the 3PCF. The algorithm is further generalized in section 5 to compute correlation functions of arbitrary order in a k -dimensional space. Section 6 is devoted to address the speed and efficiency of the overall performance, as well as the accuracy, with empirical performance results from 3PCF computations. Finally, we review all the procedures taken to compute the correlation functions, and conclude with potential applications of the method in section 7.

2 Build Tree in 2D

We use the monopole bisectional binary tree described in Pen (2003) and node-to-node interactions to compute the n -PCF.

The tree needs be constructed only once, and remains useful thereafter for computing correlation functions of arbitrary order. For this reason, we should invest sufficient computing resources into this step to minimize the worst case error arising from the utilization of the tree method. In order to achieve this, we exploit a monopole tree decomposition.

One starts by defining a 'root' node which contains all particles. For nodes where only one particle is present, we simply store the information about that particle with the node. We never subdivide a single-particle node.

For any node containing more than one particle, the longest node extent is defined as the line joining the weighted centre of mass (COM) and the particle furthest from the COM; the length of the longest node extent is called the size of the node. We orthogonally project all the particles onto the longest node extent, and choose the 'projected median point' to be a point on the line which divides the longest node extent evenly in the following sense. In the case where the number of particles in the node is even, the 'projected median point' divides the longest node extent into two rays which contain an equal number of projected particles; otherwise, the particles in one ray would outnumber those in the other ray by exactly one. When it is necessary to subdivide the node, we spatially separate the node into two subnodes by a cut perpendicular to the longest node extent and through the 'projected median point'. This method of partitioning space is demonstrated for a sample of seven points in figure 1. When walking the tree, the size of a node is a crucial piece of information for the 'open angle' test to be discussed in section 3.1.2.

For a data set containing N particles where N is an integer power of 2, we always find an exactly equal number of particles in all nodes situating at the same level of the tree hierarchy; otherwise, it is possible for a minority (ie. less

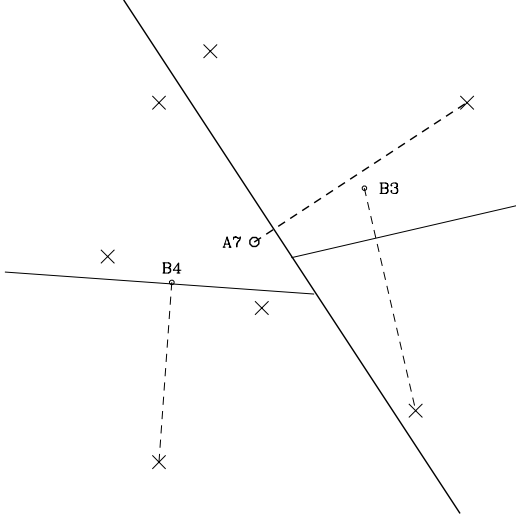


Fig. 1. For a set of seven points, we first find the weighted average position; in this plot, it is simply the centre of mass, labeled by A7, because we choose equal weight for each point. We subdivide the root node by cutting through a projected median point perpendicular to the line connecting the weighted centre of mass and the furthest particle from it, that is, the dashed line emitting from A7. We then recursively subdivide each of the daughter nodes in the same manner. The character-number labels in this figure indicate the placement of the nodes, whose centres of mass coincide with the small circles, in the tree hierarchy, as shown in figure 2.

or equal to half) of the nodes to contain one fewer particle than the other nodes at the same level. The bisectional binary tree constructed for seven particles is populated as shown in figure 2. The resulting binary tree is balanced, and the depth of the tree is pre-determined to be $1 + \log_2 N$ rounded up to the next integer. This tree is fast to build. At each level of the tree, the sorting and bisection only costs $O(N \log N)$ time for N particles. Since there are $\sim \log_2 N$ levels in the tree, the total cost of building the tree is $O(N(\log N)^2)$.

We keep track of the position of a node in the hierarchical tree structure by using an index lookup table. The index lookup table is a $(2N - 1) \times 2$ array, intended to contain the indices of the two subnodes for each of the $2N - 1$ non-empty nodes. A node is either a leaf, when it contains a single particle, or a compound node, if it is composed of two distinct subnodes. We reserve the first N rows of the table for the N leaves, numbered in the order of input, and assign to their entries the value of their own index. The next $N - 1$ rows carry indices of the subnodes belonging to the remaining $N - 1$ compound nodes which are numbered dynamically from the 'root' down during the process of tree building. In general, the entries in the i^{th} row of the table hold the indices of the two daughter nodes of the i^{th} node. Near the bottom of the tree where

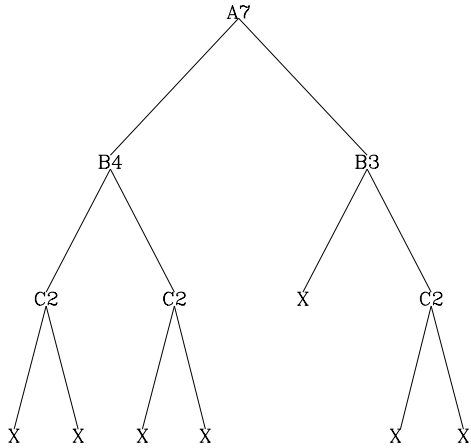


Fig. 2. The figure shows the population of a bisectational binary tree constructed for seven particles. The number at each node indicates the number of particles occupying that node. We draw our tree upside down following the convention of computer scientists. In our discussions, A is called the 'root' node and X the leaves; thus, descent means moving from the root toward the leaves.

a node contains a leaf as one of its subnodes, the corresponding entry in the index lookup table yields an index smaller than N , thus pointing back to the first N rows of the table. When walking the tree, the relation that the index of a node is smaller than N is often interpreted as a terminating signal for subdivisions which we will discuss further in section 3.1.

The weight of a compound node is the sum of the weights of its member particles. For the purpose of weak lensing data analysis, we choose the weight of a particle, ie. a galaxy, to be the inverse noise squared. For a single-particle node, the size of the node is the same as that of the particle. The particle size only has to be small enough so that it does not interfere with the 'open angle' test, and nonzero for numerical stability. Hence, we treat the particle roughly like a point, with a small but nonzero extent of $10^{-5} \times 0.2''$. This size is much smaller than $2''$ which is the minimum separation resolved by the survey, or in other words, the smallest distance between any non-degenerate pair galaxies.

We summarize the useful information to be stored in each indexed node as follows:

- the weighted centre of mass
- the size of the node
- the weight of the node
- other weighted average quantities of interest.

3 Two-Point Correlation Function

The two-point correlation function has a wide range of applications, including that in weak gravitational lensing data analysis. It can be computed cheaply, and is relatively easy to obtain from lensing surveys. Here, we discuss a node-node 2PCF construction. This approach is different from the 2PCF computation by Pen et al. (2003) which is $O(N \log N)$ and particle-node based. This node-node method costs $O(N\theta_c^{-2})$ once the tree has been built (see section 6.2 for derivation). For a flat survey geometry, the two-point correlation function can be computed rapidly using Fourier Transforms with computing time $O(N \log N)$. However, since the geometry of the sky is non-Euclidean, we cannot apply the FFT method to the problem (except as noted by Padmanabhan et al. (2003)). Then the geometry-independent 2PCF algorithm presented in this section, whose computing cost has a similar N -dependence as the FFT method though with a larger prefactor, becomes a favourable alternative. This 2PCF algorithm makes use of the bisectional binary tree constructed in section 2.

3.1 Subdivision for 2PCF

In the mainstream subdivision, we decide which pairs of nodes should be correlated. Once a pair of nodes is put into this category, we then determine whether they can be directly used to compute the two-point correlation. In the case where the nodes are sufficiently far apart from each other compared to their size, we directly correlate between them; otherwise, we further subdivide these nodes, and compare their subnodes *instead*. As noted by Barnes and Hut (1989), hierarchical methods are based on the observation that, when calculating the interaction between particles, it makes sense to ignore the detailed internal structure of distant groups of particles. More radical than using particle-group interactions, we adopt group-group interactions for distant groups in place of many particle-particle interactions between the groups. Utilizing the tree-shaped data structure, the computation of the n -PCF, which boils down to a great number of particle interactions, can be achieved with very significant computational savings.

When we come to a node, the situation is analogous to the dilemma where two people come to a three-way intersection, and must keep going forward. If we label the streets that are in front of them s_1 and s_2 , and themselves q_1 and q_2 , all possibilities of subsequent actions can be summarized as

$$\begin{aligned} q_1, q_2 &\rightarrow s_1 \\ q_1, q_2 &\rightarrow s_2 \end{aligned}$$

$$\begin{aligned}
q_1 &\rightarrow s_1, q_2 \rightarrow s_2 \\
q_1 &\rightarrow s_2, q_2 \rightarrow s_1.
\end{aligned}$$

If the persons are indistinguishable, the last two possibilities appear to be the same, then the number of different combinations is reduced from four to three. In our language, the nodes are equivalent to the persons, and the paths through which the nodes are processed are analogous to the streets. Both the mainstream subdivision and subsequent processings are independent of the ordering of arguments, which implies that the correlation between each pair would be undesirably weighted twice if the nodes were considered distinct. Hence, for our purpose, any two nodes are considered indistinguishable with respect to the subdivision process.

All possibilities can be accounted for by using a recursive subroutine called SUBDIVIDE2 which takes two input arguments indicating the indices of the nodes to be compared. Let us name the two input nodes p_1 and p_2 , and their subnodes p_1^j and p_2^j respectively, where $j \in \{1, 2\}$ labels the two subnodes. We shall refer to the indices of these nodes as k_1 and k_2 , and those of the subnodes k_1^j and k_2^j . We initiate the subdivision process by calling SUBDIVIDE2($N + 1, N + 1$) which correlates all particles within the 'root' node with index $N + 1$. Then the recursive subdivisions take over and complete the rest of the necessary subdivisions for us.

3.1.1 Mainstream subdivision

In what we call the mainstream subdivision, we correlate *between* and *within* nodes at every level of the tree hierarchy to ensure full coverage of space and separation lengths.

Case1 \Leftrightarrow SUBDIVIDE2($k_1, k_2 | k_1 = k_2$): If we want to correlate within a node, such as the 'root' node, we call SUBDIVIDE2 with $k_1 = k_2$, each of which equals the index of the node. In this case, we only have three ways of choosing two points from its subnodes, all of which should be explored:

- Choose 2 points from p_1^1 if $k_1^1 > N$
 \Leftrightarrow SUBDIVIDE2(k_1^1, k_1^1),
- Choose 2 points from p_1^2 if $k_1^2 > N$
 \Leftrightarrow SUBDIVIDE2(k_1^2, k_1^2),
- Choose 1 point from p_1^1 and 1 from p_1^2
 \Leftrightarrow SUBDIVIDE2(k_1^1, k_1^2).

Note that $k_1 = k_2$ are always greater than N by construction. The first two possibilities lead back to *Case1* at the next level. However, the third option pipes the subnodes to the further subdivision process since it explicitly specifies two distinct nodes to correlate *between*.

3.1.2 Further subdivision

Case2 \Leftrightarrow SUBDIVIDE2($k_1, k_2 | k_1 \neq k_2$): When the two arguments of SUBDIVIDE2 are different, implying $p_1 \neq p_2$, we are admitted into the further subdivision process, which depends on the 'open angle' criterion. In this step, we want to decide whether this pair of nodes is suitable to be used in computing the two-point correlation. The 'critical open angle' θ_c is an accuracy parameter that controls the further subdivision process. We define, for example, the open angle of node 1 relative to node 2 as the ratio of the size of node 1, r_1 , to the distance between the nodes, d . If this ratio, $\frac{r_1}{d}$, is greater than the critical angle θ_c , then node 1 is considered too large to be used as a unit, and we subdivide it into its two subnodes. We refer to this test as the 'open angle criterion'. As described above, the 'critical open angle', θ_c is the *maximal tolerable* ratio of the size of one node to its distance from the other node, to be satisfied by any pair of nodes being correlated. This is similar to the concept of truncation error in numerical simulations. Geometrically, θ_c represents the critical linear angle as seen from the particle we are testing². Given a pair of nodes, p_1 and p_2 , let r_i denote the size of p_i and d the separation distance between p_1 and p_2 . If both nodes meet the 'open angle' criterion, we perform the node-to-node two-point correlation (2PC) on them; otherwise, we subdivide the nodes into subnodes until each node in a pair formed by the subnodes satisfies the criterion. Each round the further subdivision is invoked, we only check whether the *first* node satisfies the 'open angle' criterion. However, both nodes should be tested before 2PC is performed on them. This is achieved by interchanging the order in which the pair of nodes is passed to SUBDIVIDE2 once the first node has met the criterion. To prevent infinite interchanges of the arguments and repeated calls of SUBDIVIDE2 even when both nodes have satisfied the criterion, we introduce a counter c , which is initially set to zero, to keep track of the number of times the criterion has been fulfilled by a node from the same pair. This is put into code format as follows with the additional argument c .

In SUBDIVIDE2(k_1, k_2, c) with $k_1 \neq k_2$:
If $\frac{r_1}{d} \leq \theta_c$ or $k_1 \leq N$, we have

```
If (c=1) then
    call 2PC(k1,k2)
    return
Else
    call SUBDIVIDE2(k2,k1,c+1)
Endif.
```

² The concept of the 'open angle' and some advantages of the tree scheme in terms of solving the gravitational N -body problem have been thoroughly explained by Barnes and Hut (1989).

If $\frac{r_1}{d} > \theta_c$ and if $k_1 > N$, we subdivide p_1 , and correlate between all pairs formed by p_2 and a subnode of p_1 by carrying out the following actions.

Choose 1 points from p_1^1 and 1 from p_2

\Leftrightarrow SUBDIVIDE2($k_1^1, k_2, c = 0$),

Choose 1 points from p_1^2 and 1 from p_2

\Leftrightarrow SUBDIVIDE2($k_1^2, k_2, c = 0$).

We set the counter to zero when a new pair is to be considered. During these accuracy-dependent further subdivisions, we do not compare subnodes belonging to the same parent node as this would interfere with the duty of the mainstream subdivision. All pairs of nodes satisfying the 'open angle' criterion are sent to the node-to-node two-point correlation (2PC) discussed in the next section.

The combined subdivision process is designed such that, when θ_c is assigned a sufficiently small value, all pairs of individual particles are taken into account, as in the brute force approach, to yield the exact 2PCF.

3.2 Node-to-node two-point correlation in 2D

In the subroutine 2PC, given a pair of distinct nodes, we add the product of their weighted field quantities and that of their weights to the respective accumulated sums binned according to the pair separation. The final 2PCF is obtained by taking the quotient of these two sums, and should be independent of the field orientation. In weak lensing analysis, both scalar fields, eg. $\kappa(\mathbf{X})$, and spin-2 fields, eg. $\gamma(\mathbf{X})$, are frequently encountered. The 2PC for a scalar field is straight-forward. It requires a unique identification of pair configurations, regardless of its orientation in the physical space, with a suitable binning. The 2PC for a spin-2 field, however, requires additional treatment. For a spin-2 field, a coordinate change is necessary to eliminate the effect due to difference in the pair orientation, and a choice should be made about what independent components of the 2PCF are to be stored.

3.2.1 2PC for a 2D scalar field

In weak gravitational lensing, the scalar field κ , which is the projected mass density, is an important observable quantity. The computation of the two-point correlation function for such 2D scalar fields is thus a basic but essential task. Here, using the κ field as an example, we illustrate an orientation independent way to map pairs to the corresponding configuration space with a logarithmical binning.

We use a simulated projected mass density map consisting of up to a million galaxies. The quantities used for the 2PC computation are the position (x, y) , κ , and the noise for each galaxy. When analyzing weak lensing data, the weight of each individual galaxy is taken to be the inverse noise squared. Recall that in the tree construction, we sum up the weights of all galaxies in the node, and store the sum as the weight of the node. Aside from the weight and the size of a node, whose definitions are given in section 2, other quantities associated with the node are weighted averages.

The configuration space for the 2PCF in 2D is one-dimensional, and can be parameterized by the distance between the pair. For computational convenience, we logarithmically bin the separation between the pair of points. The final two point function is a one-dimensional scalar function of logarithmically binned intervals of separation distances, given by

$$\xi_2 = \frac{\tilde{\xi}_2}{\tilde{w}_2} \quad (3)$$

where, for all pairs of nodes, A and B , belonging to a given configuration interval η ,

$$\tilde{\xi}_2(\eta) = \sum \bar{\kappa}(A)\bar{\kappa}(B) \quad (4)$$

and

$$\tilde{w}_2(\eta) = \sum w(A)w(B). \quad (5)$$

In equation 4, $\bar{\kappa}$ is the weighted sum of the κ values which belong to the particles in the node. This weighted sum is obtained by multiplying the weighted average of the quantity κ at the node by the total weight of the node.

3.2.2 2PC for a 2D spin-2 field

In this section, we show how two-point correlation statistics can be accumulated when applied specifically to a spin-2 lensing shear map. We use a simulated shear map consisting of up to a million galaxies. The quantities obtained from the simulation are the position (x, y) , the shear (γ_1, γ_2) , and the noise for each galaxy. We continue to use the parameterization and the logarithmic binning described in the previous section. However, for a spin-2 field, we also need to perform a coordinate transformation to ensure the rotational invariance of the 2PCF.

The original coordinate system is chosen such that all galaxies have positive x and y as components of their position when the data is stored. We are free

to do so since the correlation function is invariant in translations of the coordinate system. The shears are conventionally recorded as (γ_1, γ_2) in Cartesian coordinates, like that in our simulation. However it can also be expressed in polar coordinates as (γ, ϕ) . The conversions between these two bases are

$$\gamma_1 = \gamma \cos 2\phi, \quad (6)$$

$$\gamma_2 = \gamma \sin 2\phi \quad (7)$$

and

$$\gamma = \sqrt{\gamma_1^2 + \gamma_2^2}, \quad (8)$$

$$\tan(2\phi) = \frac{\gamma_2}{\gamma_1}. \quad (9)$$

Here, we correlate the shear components in terms of a special angular coordinate. For any two points, A and B , we first convert each of their shears given as (γ_1, γ_2) into the polar components (γ, ϕ) . While keeping γ fixed at each point, we subtract from their original ϕ the angle $\beta \in \{0, \pi\}$ between $\hat{\mathbf{x}}$ and the line connecting the two points. We then convert the rotated shears back into Cartesian coordinates, and denote them as (γ'_1, γ'_2) . These rotated shears are used to compute the two-point correlation function.

The 2PCF of a spin-2 field in 2D has two *independent* components. We choose to keep track of the quantities ξ_+ and ξ_- , which are defined below, as the two components of the two-point function. Therefore,

$$\xi_2 = (\xi_+, \xi_-) \quad (10)$$

where

$$\xi_{\pm} = \frac{\tilde{\xi}_{\pm}}{\tilde{w}_2} \quad (11)$$

and for all pairs of nodes, A and B , with a separation distance falling within the logarithmically binned configuration interval η ,

$$\tilde{\xi}_+(\eta) = \sum \bar{\gamma}_1(A)\bar{\gamma}_1(B) + \bar{\gamma}_2(A)\bar{\gamma}_2(B), \quad (12)$$

$$\tilde{\xi}_-(\eta) = \sum \bar{\gamma}_1(A)\bar{\gamma}_1(B) - \bar{\gamma}_2(A)\bar{\gamma}_2(B), \quad (13)$$

$$\tilde{w}_2(\eta) = \sum w(A)w(B). \quad (14)$$

In these equations, $(\bar{\gamma}_1, \bar{\gamma}_2)$ is the weighted sum of (γ'_1, γ'_2) for the galaxies contained in the node, weighted by their inverse noise squared, and w denotes the weight of the node. ξ_{\pm} and \tilde{w}_2 are the raw correlation functions which are binned by the pair separation. ξ_+ and ξ_- do not depend on the ordering of the two points but only on the rotationally invariant spatial configuration which is the separation distance between the two points in the case of the 2PCF. The final two point function has two-components, and is stored on a one-dimensional grid which corresponds to logarithmically binned intervals of separation distances.

4 Three-Point Correlation Function

In weak lensing, the three-point function is an important tool for detecting the non-Gaussianity in dark matter distribution, which is in turn used to break the $\Omega - \sigma_8$ degeneracy. However, the three-point correlation function is computationally more complex. At face value, the 3PCF would appear to be an $O(N^3)$ operation. Such high computational cost makes it prohibitively expensive to compute the full 3PCF for a large number of particles, eg. $\sim 10^5$ galaxies that are in a single field of our current lensing maps. Fortunately, based on similar principles as the 2PCF computation, we are able to compute the 3PCF in $O(N\theta_c^{-4} \ln(\theta_c^2 N))$ time (see section 6.2 for derivation).

4.1 Subdivision for 3PCF

Since we use a *binary* tree to compute the *three* point function, the subdivision process can become tricky. As in the subdivision process for the 2PCF described in section 3.1, we break up our discussion of the 3PCF subdivision into two parts: the mainstream subdivision and the accuracy-dependent further subdivision. The algorithm flows only from the mainstream subdivision to the further subdivision, but never in the opposite direction. This is strictly a one-way traffic because the triplets of nodes, which leave the mainstream subdivision, indicate areas amongst which correlation statistics must be taken; whereas, the further subdivision is used only to correlate these nodes up to a certain accuracy level.

To summarize the whole subdivision process in a systematic way, we construct a recursive subroutine named SUBDIVIDE3 with three input arguments which are the indices of the three nodes being compared, not necessarily distinct. Let the current arguments be denoted by k_1, k_2 and k_3 , which are the indices of the nodes p_1, p_2 and p_3 respectively; and we write the subnodes of p_i as p_i^1 and p_i^2 , with indices k_i^1 and k_i^2 . Similar to the 2PCF, we only need to initiate

the process by explicitly calling $\text{SUBDIVIDE3}(N + 1, N + 1, N + 1)$ once in the main program where $N + 1$ is the index of the root node; this correlates among any three patches of area within the root node. Then the rest of the processings are neatly taken care of by recursions.

4.1.1 Mainstream subdivision

The mainstream subdivision ensures that correlations are performed *on* and *amongst* all areas of the map. We again begin from the root node and move down the tree. At the root level, when $\text{SUBDIVIDE3}(N + 1, N + 1, N + 1)$ is invoked, the three arguments correspond to a single patch of area, thus we can only perform 'internal correlations' by subdividing the 'root' node and comparing the subnodes. However at the next level, two of the arguments may be distinct, in which case we can do both 'internal' and 'external' correlations by examining all possible combinations formed by any three of the four immediate subnodes of the given pair of nodes. Whenever we have three distinct nodes to correlate amongst, these nodes are passed to the further subdivision procedure. We summarize all cases which may be encountered in the mainstream subdivision.

Case1 $\Leftrightarrow \text{SUBDIVIDE3}(k_1, k_2, k_3 | k_1 = k_2 = k_3)$: If we want to correlate within a node, as in the case of the root node, we call SUBDIVIDE3 with three identical arguments. This means that the input nodes are indeed the same. In this case, there are four possible ways of choosing a triplet of patches from its two subnodes, p_1^1 and p_1^2 , all of which must be explored:

- Choose all 3 points from p_1^1 if $k_1^1 > N$
 $\Leftrightarrow \text{SUBDIVIDE3}(k_1^1, k_1^1, k_1^1),$
- Choose all 3 points from p_1^2 if $k_1^2 > N$
 $\Leftrightarrow \text{SUBDIVIDE3}(k_1^2, k_1^2, k_1^2),$
- Choose 2 points from p_1^1 and 1 from p_1^2 if $k_1^1 > N$
 $\Leftrightarrow \text{SUBDIVIDE3}(k_1^1, k_1^1, k_1^2),$
- Choose 2 points from p_1^2 and 1 from p_1^1 if $k_1^2 > N$
 $\Leftrightarrow \text{SUBDIVIDE3}(k_1^2, k_1^2, k_1^1).$

The first two possibilities correspond to correlations within each of the subnodes while the last two indicate correlations between the two subnodes. Notice that in the last two possibilities, whenever SUBDIVIDE3 is invoked with exactly two distinct arguments, the arguments are ordered such that the first two are identical for coding simplicity. Recursively calling SUBDIVIDE3 in this manner divides the flow at each level. Where the three arguments are identical, as in the first two possibilities, we repeat the same procedure as for a single node described above; however, the last two possibilities lead us to *Case2*.

Case2 \Leftrightarrow SUBDIVIDE3($k_1, k_2, k_3 | k_1 = k_2 \neq k_3$): When the arguments involve exactly two distinct nodes, the first two arguments are always the same and the last different by construction. With this setup, we can easily determine the stage of flow by checking the logical relations between adjacent arguments. If $k_1 = k_2$ and $k_2 \neq k_3$, this means that we intend to consider the correlation among any three points with two points selected from p_1 and one from p_3 . Since the purpose of the mainstream subdivision is to specify three distinct regions from where each point in a triplet should be selected from, and we must choose exactly one point from p_3 , it makes no difference other than increasing the computational cost to further subdivide p_3 , which corresponds to specifying the region in p_3 from where that one point is chosen from. Whenever p_1 contains more than one particle, which is ensured by construction, we subdivide it in each of the following three ways:

Choose 2 points from p_1^1 and 1 from p_3 if $k_1^1 > N$
 \Leftrightarrow SUBDIVIDE3(k_1^1, k_1^1, k_3),
 Choose 2 points from p_1^2 and 1 from p_3 if $k_1^2 > N$
 \Leftrightarrow SUBDIVIDE3(k_1^2, k_1^2, k_3),
 Choose 1 point from p_1^1 , 1 from p_1^2 , and 1 from p_3
 \Leftrightarrow SUBDIVIDE3(k_1^1, k_1^2, k_3).

The subroutine SUBDIVIDE3 is recursively invoked with the appropriate argument sets as indicated. The first two possibilities bring us back to *Case2* while the third breaks into further subdivision since three distinct nodes are specified. Recursively performing the mainstream subdivisions ultimately covers correlations over the entire map, and eventually breaks down the 'root' node into distinct triplets of nodes which must be correlated amongst. These triplets are subsequently delivered to the further subdivisions.

4.1.2 Further subdivision

Case 3 \Leftrightarrow SUBDIVIDE3($k_1, k_2, k_3 | k_1 \neq k_2 \neq k_3$): If the arguments of the SUBDIVIDE3 subroutine are pairwise distinct, the three input nodes are tested on if they are able to contribute accurate enough three-point correlation statistics, or need be further subdivided. As in the 2PCF, the further subdivision does not call for the collection of three-point statistics until the 'open angle' criterion introduced in section 3.1.2 has been met by all three nodes. The only subtleties are that the 'open angle' criterion must now be satisfied by two ratios at each node, and that the possible ways of failure are more varied for the 3PCF further subdivision.

Instead of checking all ratios for all three nodes every time the further subdivision is called, we simply check the 'open angle' criterion for the first node. All other nodes are checked by calling further subdivision with the input nodes in

rotation once the current node has satisfied the criterion. We keep a counter c , initially set to zero, to indicate the number of times the 'open angle' criterion has been consecutively satisfied; when $c = 2$, we call for the node-to-node three-point correlation, shorthanded 3PC, with the three distinct nodes as arguments. Checking the criterion before each node is subdivided ensures that only the minimal number of necessary further subdivisions are performed.

Any three input nodes, p_1 , p_2 and p_3 , form a triangle, non-degenerate or degenerate. We shall call this triangle $\triangle ABC$, whose vertices are labeled in the order of the input nodes, and their opposite sides a , b and c . We let r_1 represent the size of p_1 , and let p_1^1 and p_1^2 denote its subnodes. In further subdivisions, we must choose one point from each input node.

If $\max(\frac{r_1}{b}, \frac{r_1}{c}) \leq \theta_c$, then p_1 satisfies the criterion and does not need be subdivided; however, before we can call 3PC amongst these three nodes, we must also check whether the other two nodes satisfy the 'open angle' criterion if we have not already done so. If any of the nodes in the triplet has not been tested $\Leftrightarrow c < 2$, we call SUBDIVIDE3 with the nodes in a rotated order such that in the next round, we examine a different node which is labelled p_2 currently. Rotating the same triplets three times completes a full rotation. Therefore, $c = 2$ implies that the other two nodes in the current configuration have already passed the 'open angle' test, and since the current node also satisfies the criterion, we can use this triplet to compute the 3PCF by calling the subroutine 3PC where the raw correlation functions are accumulated. This is put into pseudo-code below.

In SUBDIVIDE3(k_1, k_2, k_3, c) with $k_i = \delta_{ij}k_j$:

If $\max(\frac{r_1}{b}, \frac{r_1}{c}) \leq \theta_c$ or $k_1 \leq N$, we have

```

If c=2 then
  call 3PC(k1,k2,k3)
  return
Else
  call SUBDIVIDE3(k2,k3,k1,c+1)
Endif.

```

If $\max(\frac{r_1}{b}, \frac{r_1}{c}) > \theta_c$ and $k_1 > N$, we subdivide p_1 by taking the following actions.

```

Choose 1 point from  $p_1^1$  and 1 each from  $p_2$  and  $p_3$ 
 $\Leftrightarrow$  SUBDIVIDE3( $k_1^1, k_2, k_3, c = 0$ ),
Choose 1 point from  $p_1^2$  and 1 each from  $p_2$  and  $p_3$ 
 $\Leftrightarrow$  SUBDIVIDE3( $k_1^2, k_2, k_3, c = 0$ ).

```

We reset the counter c to be zero in the case where a different triplet configuration will be examined, for example, when one of the nodes is subdivided. When

the triplet passes the 'open angle' test, it is subsequently sent to the node-to-node three-point correlation described in the next section. In summary, the accuracy-dependent further subdivision serves the sole purpose of accumulating *accurate enough* statistics amongst the three different area patches covered by the triplets of distinct nodes leaving from the mainstream subdivision.

Similar to the 2PCF, this subdivision process will count all $\binom{N}{3}$ triplets

when θ_c is set to zero. This is a $O(N^3)$ process as in the computation of the 3PCF by definition, and is prohibitively expensive for N of astronomical interest. The accuracy parameter θ_c controls the depth of subdivision and makes this otherwise intractable calculation feasible. One expects the truncation error from tree walking to scale as θ_c^2 . For a comparison between the 3PCF computed using our fast algorithm with nonzero θ_c and the fully accurate results obtained using the brute force approach, refer to section 6.

4.2 Node-to-node three-point correlation in 2D

The subroutine 3PC computes the raw correlation functions for the weighted field quantities and for the weights using triplets of distinct nodes that exit the subdivision procedure. These correlation functions are then used to compute the final 3PCF which is the quotient of the two raw functions. Here, we describe the node-to-node three-point correlation procedure for both 2D scalar fields and spin-2 fields.

We consider the information about each node, obtained while building the tree, to be concentrated at its weighted centre of mass; thus, we may consider the nodes point-like in the following discussion.

4.2.1 3PC for a 2D scalar field

The 3PCF for a scalar field is a scalar function of triangle configurations, defined on a three-dimensional grid. The 3PC for a scalar field relies on a map from the space of triangles to the three-dimensional configuration space, which does not assume parity, as a parameterization of triangle configurations. Here, we describe the procedure of node-to-node three-point correlation for the scalar field κ .

We measure the position of the galaxies in Cartesian coordinates, their projected mass density κ and the noise. For any triplet $\{p_1, p_2, p_3\}$ entering the 3PC subroutine, we define the sides a, b, c , and their opposite vertices A, B, C for the triangle formed by the triplet as follows. Given any three points,

we first identify the longest side and name it a . We then name the other two sides b and c in the counter-clockwise direction.

For numerical reasons, we discretize the finite region of the configuration space accessible to triplets in the system into finitely many 3-dimensional rectangles η by logarithmically binning each of the length dimensions. Therefore, the three-point function ξ_3^κ is given by the quotient of the raw correlation functions as

$$\xi_3^\kappa = \frac{\tilde{\xi}_3^\kappa}{\tilde{w}_3} \quad (15)$$

where, for all triplets $\{A, B, C\}$ with coordinates $(s_1, s_2, s_3) \in \eta$ in the configuration space, which are the lengths of the sides a , b and c respectively, and $\bar{\kappa}$ the weighted sum of κ at the node,

$$\tilde{\xi}_3^\kappa(\eta) = \sum \bar{\kappa}(A)\bar{\kappa}(B)\bar{\kappa}(C) \quad (16)$$

and

$$\tilde{w}_3(\eta) = \sum w(A)w(B)w(C). \quad (17)$$

In weak lensing, $\kappa(\mathbf{X})$ is the projected matter overdensity. To calculate the skewness in the projected dark matter distribution from the three point function of κ , ξ_3^κ , we adopt the compensated Gaussian filter U used in Pen et al. (2003) as the smoothing window function for κ , which gives

$$\langle \bar{\kappa}^3 \rangle = 2\pi \int \xi_3^\kappa(r, \mathbf{X}) U_3(r, \mathbf{X}) r dr d^2x. \quad (18)$$

To accommodate our choice of coordinates, with (s_1, s_2, s_3) being the length of a , b and c respectively, we obtain

$$\begin{aligned} \langle \bar{\kappa}^3 \rangle &= 4\pi \int_0^\infty \int_0^\infty \int_{|s_1-s_2|}^{|s_1+s_2|} \xi_3^\kappa(s_1, s_2, s_3) U_3(s_1, s_2, s_3) \\ &\times \frac{s_1 s_2 s_3 ds_3 ds_2 ds_1}{\sqrt{-s_3^4 - s_2^4 - s_1^4 + 2s_2^2 s_3^2 + 2s_1^2 s_3^2 + 2s_1^2 s_2^2}}. \end{aligned} \quad (19)$$

4.2.2 3PC for a 2D spin-2 field

The 3PCF for a spin-2 field is conventionally a function with eight components defined on a three-dimensional configuration space. In addition to the

parameterization of triangles, there is an orthogonal transformation involved in the 3PC for a spin-2 field.

We measure the position of the galaxies in Cartesian coordinates, their projected mass density κ and the noise. The three-point correlation statistics for each triplet is obtained after a coordinate change for the *ordered* triplet, hence it is dependent upon the ordering of the points. To reduce the complexity of the problem, for any triplet $\{p_1, p_2, p_3\}$ entering the 3PC subroutine, we define the sides a, b, c , and their opposite vertices A, B, C for the triangle formed by the triplet in the same way as in section 4.2.1 for a scalar field. Recall that we define $\triangle ABC$ by first identifying the longest side as a , and the other two sides b and c in the counter-clockwise direction.

Similarly, we choose (s_1, s_2, s_3) , which are the lengths of a, b and c respectively, as the coordinates in the configuration space while each spatical dimension is binned logarithmically to give finitely many 3-dimensional rectangles η in the configuration space.

Since we are interested in the 3PCF for the spin-2 field relative to the configuration rather than to any fixed spatial coordinates, we need to project γ onto a coordinate system intrinsic to the ordered triplet $\{A, B, C\}$. Let $\hat{\mathbf{x}}'$ be the unit vector $\widehat{\mathbf{BC}}$, and $\hat{\mathbf{y}}'$ the unit vector which is perpendicular to $\hat{\mathbf{x}}'$ and points from line segment connecting B and C to the point A . We want to obtain an expression for γ in terms of these new coordinates. Suppose γ is a spin-1 object, then the projections of γ onto $\hat{\mathbf{x}}'$ and $\hat{\mathbf{y}}'$ are simply γ'_x and γ'_y respectively with

$$\gamma'_x = \gamma \cdot \hat{\mathbf{x}}' \quad (20)$$

and

$$\gamma'_y = \gamma \cdot \hat{\mathbf{y}}'. \quad (21)$$

However, our γ is a spin-2 object. To compute its projection, it is necessary to introduce the matrix $\mathbf{\Gamma}$ defined as

$$\mathbf{\Gamma} = \begin{pmatrix} \gamma_1 & \gamma_2 \\ \gamma_2 & -\gamma_1 \end{pmatrix}. \quad (22)$$

The projected shear is given by $\gamma' = (\gamma'_1, \gamma'_2)$ where

$$\gamma'_1 = \frac{1}{2}((\hat{\mathbf{x}}')^T \mathbf{\Gamma} \hat{\mathbf{x}}' - (\hat{\mathbf{y}}')^T \mathbf{\Gamma} \hat{\mathbf{y}}') \quad (23)$$

and

$$\gamma'_2 = \frac{1}{2}((\hat{\mathbf{x}}')^T \mathbf{\Gamma} \hat{\mathbf{y}}' + (\hat{\mathbf{y}}')^T \mathbf{\Gamma} \hat{\mathbf{x}}'). \quad (24)$$

Here, $\hat{\mathbf{x}}'$ and $\hat{\mathbf{y}}'$ are taken to be unit *column* vectors. Notice that $|\gamma'| = |\gamma|$ since the transformation is orthogonal.

Recall that the weight of each node, w , is the sum of of the weights of all galaxies in the node; and the weight of a galaxy is its inverse noise squared. We compute the raw three point functions for the weight, \tilde{w}_3 , as well as for the eight components of the 3PCF, $\tilde{\xi}_{111}$, $\tilde{\xi}_{112}$, $\tilde{\xi}_{121}$, $\tilde{\xi}_{211}$, $\tilde{\xi}_{122}$, $\tilde{\xi}_{221}$, $\tilde{\xi}_{212}$ and $\tilde{\xi}_{222}$, defined as

$$\tilde{w}_3(\eta) = \sum w(A)w(B)w(C) \quad (25)$$

and

$$\tilde{\xi}_{ijk}(\eta) = \sum \tilde{\gamma}_i(A)\tilde{\gamma}_j(B)\tilde{\gamma}_k(C) \quad (26)$$

for all triplets $\{A, B, C\}$ belonging to the set of configurations η , that is $(s_1, s_2, s_3) \in \eta$. In the equations, $(\tilde{\gamma}_1, \tilde{\gamma}_2)$ represent the weighted sum of (γ'_1, γ'_2) at the node. The final three-point correlation function ξ_3 with eight components is the quotient of the raw correlation functions $\tilde{\xi}_{ijk}$ for the components and \tilde{w}_3 for the weight, that is

$$\xi_3 = \{\xi_{ijk}\} \quad (27)$$

with each component

$$\xi_{ijk} = \frac{\tilde{\xi}_{ijk}}{\tilde{w}}. \quad (28)$$

The 3PCF for a two-dimensional spin-2 field is a eight-component function defined on a three-dimensional grid corresponding to the logarithmically binned configuration space (s_1, s_2, s_3) .

5 n-point correlation function in k dimensions

The algorithm for the 2PCF and the 3PCF can be easily extended to n -th order. In this section, we discuss how the n -point correlation function can

be computed for a k -dimensional scalar field. The binary tree construction is entirely independent of the order of the correlation function. Although the subdivision process needs be generalized for higher order correlation functions (ie. n -dependent), its structure is independent of the field dimension (ie. k -independent). The k -independence of the subdivision is supported by the fact that once the tree has been constructed, the subdivision process relies on the *binary* structure of the tree rather than on the spatial structure of the particles. The node-to-node n -point correlation (n -PC) for a scalar field relies on a unique counting of n -sided polygons in a k -dimensional space.

5.1 Build tree in k dimensions

In a k -dimensional space, the tree construction is virtually the same as that in 2D. At each node p which contains more than one particle, we find the weighted centre of mass, \mathbf{X}_c , and determine among all particles in the node the one that is furthest from \mathbf{X}_c , ie. the particle with position vector \mathbf{X}_{max} such that $\|\mathbf{X}_{max} - \mathbf{X}_c\| = Sup\|\mathbf{X} - \mathbf{X}_c\|$ for all $\mathbf{X} \in p$. We then bisect the node by cutting along a $(k - 1)$ -dimensional subspace, or affine space, which is perpendicular to the line connecting \mathbf{X}_{max} and \mathbf{X}_c , and through a projected median point on this line determined as in section 2. Similar to the 2D case, the binary tree remains useful for computing the n -point correlation function where n is any positive integer no greater than N .

5.2 Subdivision for n -PCF

The subdivision process for computing the n -point correlation function can be divided into two parts as with the 2PCF and the 3PCF, and be dealt with in a single recursive subroutine SUBDIVIDE which takes n arguments. The mainstream subdivision occurs when the input nodes are not pairwise distinct; otherwise, the θ_c -dependent further subdivision is performed. The subroutine SUBDIVIDE(**nodes**, n , c), where **nodes** is a 1D array of length n containing the indices of the n input nodes, is discussed below.

5.2.1 Mainstream subdivision

\Leftrightarrow SUBDIVIDE($k_1, \dots, k_n | k_i = k_j$ for some $i \neq j$):

If the n elements of **nodes** are not pairwise distinct, we want to call SUBDIVIDE with all possible combinations, formed by the non-repeating nodes and the subnodes of the repeating ones, as input argument sets. Interested readers should see the appendix for an outline of the n -PCF mainstream subdivision scheme. We call SUBDIVIDE in such a way as to keep the repeating nodes

together. This specific ordering allows us to easily determine whether a set of nodes is pairwise distinct and find the repeated ones by checking only the adjacent nodes.

5.2.2 Further subdivision

\Leftrightarrow SUBDIVIDE($k_1, \dots, k_n | k_i \neq k_j$ for any $i \neq j$):

When all n input nodes are pairwise distinct, further subdivision of the first node p_1 is performed upon the condition that the 'open angle' criterion is not satisfied by p_1 . The 'open angle' criterion for p_1 , in the n -th order case, is the condition that $\max(\frac{r_1}{d_i}) \leq \theta_c$ where r_1 is the size of p_1 , and d_i for $i \in \{2, \dots, n\}$, is the separation distance between p_1 and p_i . Whenever p_1 meets the criterion, we check whether the counter c , which keeps track of the number of points on the n -sided polygon that have passed the 'open angle' test, reads $n - 1$. If so, we accumulate n -point statistics using these nodes by calling the subroutine n -PC; otherwise, we recursively call SUBDIVIDE with the input nodes rotated by one. This process is demonstrated below.

In SUBDIVIDE(**nodes**, n , c) with $k_i = \delta_{ij}k_j$:

If $\max(\frac{r_1}{d_i}) \leq \theta_c$ or **nodes**(1) $\leq N$, we have

```

If (c=n-1) then
    call n-PC(nodes,n)
    return
Else
    call SUBDIVIDE(cshift(nodes,1),n,c+1)
Endif.

```

If p_1 does not satisfy the 'open angle' criterion and it contains distinct subnodes, we *replace* the correlation amongst the n input nodes by a pair of correlations each accounting for one of the combinations formed by a subnode of p_1 and the remaining $n - 1$ nodes. This is summarized in code format below.

In SUBDIVIDE(**nodes**, n , c) with $k_i = \delta_{ij}k_j$:

If $\max(\frac{r_1}{d_i}) > \theta_c$ and **nodes**(1) $> N$,

```

snodes=nodes
snodes(1)=nodes(1).sub1
call SUBDIVIDE(snodes,n,c=0)
snodes(1)=nodes(1).sub2
call SUBDIVIDE(snodes,n,c=0).

```

We reset the counter c to zero in the case where one of the nodes must be subdivided since a new n -tuple configuration is subsequently considered. This

way, the counter reads $n - 1$ if and only if all the other $n - 1$ nodes besides the one being examined have satisfied the 'open angle' criterion.

5.3 Node-to-node n-point correlation for scalar fields

This section includes a general discussion about the parameterization of n -tuple configurations in k dimensions (section 5.3.1) and a detailed description of how the n -PC can be done for a two-dimensional scalar field (section 5.3.2).

5.3.1 Node-to-node n-point correlation of a k -dimensional scalar field

Let us consider a single point in a k -dimensional space, the point itself is dimensionless and rotationally invariant; therefore, when a second point is placed in the system, only its distance from the first point matters. When we add a third point, for $k \geq 2$, two parameters are generally required to specify its position relative to the first two points which form a one dimensional subspace; one of the parameters can be its orthogonally projected position onto the line segment connecting the first two points, and the other can be its perpendicular distance from the line. Given three points, they may form a plane; for $k \geq 3$, specifying yet another point relative to them requires three parameters; a set of parameters could be the projected position of the fourth point onto the plane (2 parameters), and its distance from the plane (1 parameter). However, a point in a k -dimensional space cannot have more than k independent components, which sets an upper bound for the number of parameters. In general, before the i^{th} point is placed in a k -dimensional space, there pre-exists $i - 1$ points, potentially forming an object of dimension $\min(i - 2, k)$; the position of the i^{th} point in relation to the pre-existing $i - 1$ points can be specified by its orthogonal projection onto and its distance from the object formed by the first $i - 1$ points; this requires no more than $\min(i - 1, k)$ parameters. Consider forming an n -sided polygon in k -dimensional space by adding one point after another, we see that the n -sided polygon can be uniquely specified, up to rotation, by no more than m parameters where

$$m = \sum_{i=1}^n \min(i - 1, k). \quad (29)$$

Hence, the full n -point correlation function in k -dimension can be stored on a grid of dimension m defined as above.

5.3.2 Node-to-node n -point correlation of a 2D scalar field

To compute the n -point correlation function for a 2D scalar field, we follow the tree construction and subdivision as described previously. Here, we discuss how one handles the statistics for a given set of n distinct points $\{p_1, \dots, p_n\}$. We first dismiss the n -tuples with anomaly such as the coincidence of two or more points; thus, we need not consider this case in the following discussion.

We wish to find a parameterization that uniquely maps any n -tuple $\{p_1, \dots, p_n\}$ to a point in the m -dimensional configuration space, such as the parameterization suggested in section 5.3.1, with

$$m = \sum_{i=1}^n \min(i - 1, 2) \quad (30)$$

which, for $n > 1$, reduces to

$$m = 2n - 3. \quad (31)$$

For n points in two dimensions, we may order the points and parameterize the configuration as follows. We first define line l as the line joining the two points of widest separation. Let $\hat{\mathbf{y}}'$ be the unit vector perpendicular to line l and pointing towards the side with the greater number of points. We define $\hat{\mathbf{x}}'$ as the unit vector orthogonal to $\hat{\mathbf{y}}'$ such that $\hat{\mathbf{x}}'$ and $\hat{\mathbf{y}}'$ form a right-handed system. We call the point on line l with the smaller x' -component p'_1 and translate the coordinate system so that p'_1 coincides with the origin. The point on line l with the larger x' -component and coordinates $(x'_2, 0)$ in the new coordinate system is then named p'_2 . We order the other $n - 2$ points by increasing angle from the \mathbf{x}' -axis. We now have an ordered n -tuple $\{p'_1, \dots, p'_n\}$ with new coordinates $\{(x'_i, y'_i), i=1, \dots, n\}$, amongst which x'_1, y'_1 and y'_2 are zero. The ordered $2n - 3$ numbers $(x'_2, x'_3, y'_3, \dots, x'_n, y'_n)$ parameterize the m -dimensional configuration space, and are unique up to translations and rotations of the configuration.

Due to discrete nature of data storage, we partition the finite region of the m -dimensional continuous configuration space accessible to the n -tuples in the system, into finitely many m -dimensional rectangles η 's.

For all ordered n -tuples $\{p'_1, \dots, p'_n\} \in \eta$, we can compute the raw n -point function $\tilde{\xi}_n$ for the scalar field ρ , and \tilde{w}_n for the weight, as a function of discretized configuration, by

$$\tilde{\xi}_n(\eta) = \sum \left(\prod_{i=1}^n \bar{\rho}(p'_i) \right), \quad (32)$$

and

$$\tilde{w}_n(\eta) = \sum \left(\prod_{i=1}^n w(p'_i) \right) \quad (33)$$

where $\bar{\rho}$ is the weighted sum of ρ among the particles in the node.

The final n -point correlation function ξ_n is a scalar function on an m -dimensional grid given by

$$\xi_n(\eta) \equiv \langle \prod_{i=1}^n \rho(p_i^\eta) \rangle = \frac{\tilde{\xi}_n(\eta)}{\tilde{w}_n(\eta)}. \quad (34)$$

Here, $\{\mathbf{p}^\eta\} = \{(p_1^\eta, p_2^\eta, \dots, p_n^\eta)\}$ is the set of all n -tuples which are mapped to the m -dimensional rectangle η in the configuration space under the specified parameterization.

6 Accuracy and Speed in 2D

The accuracy and speed of our algorithm in 2D are analyzed in this section. We first show that tests of algorithm accuracy for the 3PCF yield results which are consistent with our expectation. We then turn to examine the algorithm speed and memory usage of the 2PCF and 3PCF computations, with focus on the computational costs of the subdivision and node-to-node correlation procedures. To do this, we offer a theoretical estimate of the computational costs, followed by results and analysis from various tests of algorithm speed. Finally, we compare the costs of our 2PCF and 3PCF algorithms with that of other correlation algorithms.

6.1 Tests of Accuracy for 3PCF

The error of the algorithm, due to the truncation error of the binary tree, is expected to scale as θ_c^2 . Here, θ_c is an accuracy parameter specifying the critical linear angle, as seen from a node p_i , above which size another node p_j cannot be treated as a unit and must be subdivided.

We test the accuracy of the algorithm in 2D 3PCF computation for $N = 1000$ using CITA's 1.3GHz ItaniumII, Dell Poweredge 7250 computer. For this set of computations, we make use of a mock catalogue of galaxies with x, y coordinates, $\gamma_1, \gamma_2, \kappa$ and noise. The positions of the galaxies are randomly generated

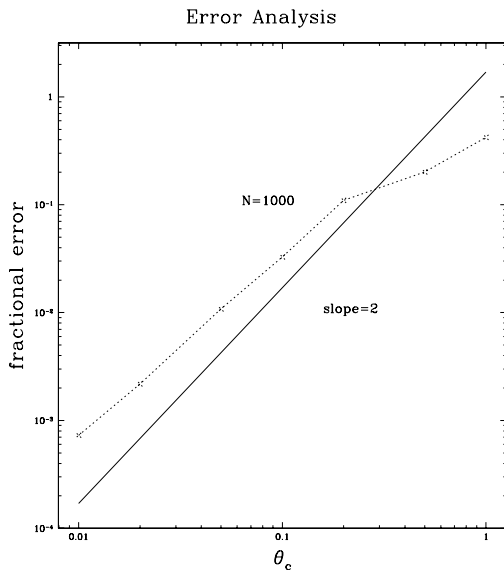


Fig. 3. For 1000 particles, we plot the fractional error of the 3PCF for a scalar field computed using the new algorithm compared to that using the brute force approach. Recall that the 3PCF is stored on a 3D grid. We first smooth over the neighbouring grids, then compute the fractional error $\Delta = \sqrt{\frac{\sum_{i,j,k} (\xi_{\theta_c} - \xi_*)^2}{\sum_{i,j,k} \xi_*^2}}$ where ξ_* is the 3PCF computed by direct summation over all triplets of particles. We see that the truncation error scales as θ_c^2 which agrees with our estimate.

with coordinate components taking values between 0 and 5. Since γ_1 and γ_2 are not used in accuracy testing, we set them to zero. For equal weighting in the 3PCF, the noise figures of the galaxies are identically assigned the value of 1. The scalar field κ assumes a two-dimensional Gaussian distribution around the centre of the map given by

$$\kappa(x, y) = \exp \left[-\frac{(x - x_0)^2 + (y - y_0)^2}{2\sigma^2} \right]. \quad (35)$$

Here, $(x_0, y_0) = (2.5, 2.5)$ are the coordinate components of the map centre, and the width of the Gaussian distribution, $\sigma = 1.25$, is a quarter of the map's side length. The 3PCF is binned at logarithmic intervals of $2^{0.5}$ over the length scale from 0.1 to $\sqrt{2} \times 5$. The higher cutoff length corresponds to the diagonal length of the 2D lensing map.

The truncation error for the 3PCF computation on a 2D scalar field using the tree approach is plotted against different θ_c in figure 3. Empirical runs show that the error is proportional to θ_c^2 as predicted in section 4.1. When $\theta_c = 0$, the fractional error is around the order of 10^{-15} , and is therefore neglectable.

In tree-based N -body simulations, typical values of the critical open angle

are $0.5 < \theta_c < 1$. Barnes and Hut (1989) find that the violation of energy conservation in a simulation using a tree-based force computation is only 2% for $\theta_c = 1$. Although the fractional error in $\langle \bar{\kappa}^3 \rangle$ differs from the fractional violation of energy conservation by definition, and that the procedures used to obtain them are quite different, the high accuracy for large θ_c in N -body simulations suggests a similar relationship in our case. The quantity of interest, $\langle \bar{\kappa}^3 \rangle$, may turn out to be accurate enough for our purpose even when θ_c is large. Furthermore, only a small subset of all triangle configurations are ever considered for most scientific questions derived from the 3PCF. As a result, the errors in the smoothed skewness fields, eg. equation 18, derived from the partial 3PCF are probably comparable to that in figure 3. Hence, it is possible that values such as $\theta_c = 0.5$ are quite sufficient for 3PCF computations.

6.2 Estimate of Computational Cost for 2PCF and 3PCF

Here, our primary goal is to provide a theoretical estimate for the cost of the 3PCF algorithm in 2D. In addition, we derive the computational cost of the 2D 2PCF at the end of the subsection.

In the brute force 3PCF computation, the computing time can be broken down into the following components, reading of the catalogue, computation of the raw correlation functions, normalization of the raw correlation functions for γ and κ by the raw weight correlation function, and finally the output of the full 3PCF. In addition to the above procedures for brute force calculations, the 3PCF computation using our fast algorithm also spends time on tree building just after reading the catalogue. Among these processes, the reading of catalogue and the output of 3PCF are considered extrinsic to the computation algorithm. In a gridded 3D configuration space, the normalization cost is independent of θ_c and N . Here, we only discuss the speed of tree building and that of the raw correlation function computation.

In 2D, the construction of the tree costs $O(N(\log N)^2)$ for N particles. In the k -dimensional case, however, building the tree costs $O(kN(\log N)^2)$ because it involves solving k components of the distances. Since the cost of the tree construction is relatively well-understood, and that its prefactor is small (see figure 4), we will focus on the cost of raw 3PCF computation in the remaining section.

In the following paragraphs, we offer a derivation for the computational cost of the raw 3PCF. We show that when $\theta_c^2 N$ is sufficiently large, the computing time scales as $N\theta_c^{-4} \ln(\theta_c^2 N)$. This slowly converges to $O(N\theta_c^{-4})$ as $\theta_c^2 N$ gets very large.

Since the isosceles and equilateral triangles constitute a set of measure zero in

the configuration space, we can neglect them from the integral used to estimate the total number of contributing triplets³. Here, we consider an arbitrary triplet of nodes forming a scalene triangle. We call the node opposite to the longest side p_1 , the node closer to p_1 p_2 , and the other node p_3 . We then label the side connecting p_i and p_j as d_{ij} , and we have $d_{ij} = d_{ji}$. Furthermore, we denote the size of p_i by r_i .

In the given triplet configuration, since $d_{12} < d_{13} < d_{23}$, the open angle criterion demands

$$\frac{r_1}{d_{13}} < \frac{r_1}{d_{12}} < \theta_c, \quad (36)$$

$$\frac{r_2}{d_{23}} < \frac{r_2}{d_{12}} < \theta_c \quad (37)$$

and

$$\frac{r_3}{d_{23}} < \frac{r_3}{d_{13}} < \theta_c. \quad (38)$$

We are only interested in triplets which would contribute to the correlation statistics. For such a triplet, if any of the nodes were replaced by its parent node, the obtained triplet would no longer satisfy the open angle criterion. Except at the bottom of the tree, the area of the parent node is expected to double that of the current node, hence the expected increment in linear node size one level up gives a factor of $\sqrt{2}$. Therefore, we obtain for contributing triplets

$$\frac{r_1}{\theta_c} < d_{12} < \sqrt{2} \frac{r_1}{\theta_c}, \quad (39)$$

$$\frac{r_2}{\theta_c} < d_{12} < \sqrt{2} \frac{r_2}{\theta_c} \quad (40)$$

and

$$\frac{r_3}{\theta_c} < d_{13} < \sqrt{2} \frac{r_3}{\theta_c}, \quad (41)$$

which then yields

$$\frac{1}{\sqrt{2}} \theta_c d_{12} < r_1 < \theta_c d_{12}, \quad (42)$$

³ We use the term 'contributing triplets' in place of 'triplets which contribute to the correlation statistics.'

$$\frac{1}{\sqrt{2}}\theta_c d_{12} < r_2 < \theta_c d_{12} \quad (43)$$

and

$$\frac{1}{\sqrt{2}}\theta_c d_{13} < r_3 < \theta_c d_{13}. \quad (44)$$

We see that the sizes of p_1 and p_2 are governed by d_{12} whereas the size of p_3 is governed by d_{13} .

Let us now fix an arbitrary node in the tree hierarchy as p_1 , and find another pair of nodes p_2 and p_3 such that they form a contributing triplet with $d_{12} < d_{13} < d_{23}$. We set up consecutive annuli centred at p_1 , outlined by concentric circles of radius which increases with a factor of $\sqrt{2}$, starting with the annulus given by $\frac{r_1}{\theta_c} < d < \sqrt{2}\frac{r_1}{\theta_c}$ where d is the distance from p_1 .

We argue in the following that the possibility of finding a node in any of these annuli, which qualifies as a member of a contributing triplet containing p_1 in the manner described above, is proportional to θ_c^{-2} . The area of the j^{th} annulus with $d_j < d < d_{j+1}$ where $d_j = 2^{\frac{j-1}{2}}\frac{r_1}{\theta_c}$ is given by

$$\pi(d_{j+1}^2 - d_j^2) = \pi d_j^2; \quad (45)$$

whereas, a qualifying node⁴ in the j^{th} annulus has an area proportional to $\theta_c^2 d_j^2$. Furthermore, nodes of similar sizes should not overlap. Thus, the possibility of finding a qualifying node in any of the annuli is θ_c^{-2} up to a constant factor which is independent of j .

As shown above, in a contributing triplet, the distance of p_2 from p_1 in terms of r_1 is given by equation 39. From equation 36 and the definition of L as the largest node separation in the image, the distance of p_3 from p_1 can also be expressed in terms of r_1 as

$$\frac{r_1}{\theta_c} < d_{13} < L. \quad (46)$$

Geometrically speaking, for a node to qualify as p_2 in such a configuration, it must fall in the first annulus. The number of different nodes, which qualify to be p_2 , is thus proportional to the possibility of finding a qualifying node in the first annulus, that is $\propto \theta_c^{-2}$ as derived above. However, p_3 can fall in any of the

⁴ We use the term 'qualifying node' in place of 'a node which qualifies as a member of a contributing triplet containing p_1 such that p_1 is the node opposite to the longest side of the triangle'.

annuli, with each annulus containing roughly θ_c^{-2} qualifying nodes. Since there are about $\ln \frac{L}{r_1/\theta_c}$ such annuli in a map with a maximum node separation L , the number of different nodes which qualify to be p_3 is proportional to $\theta_c^{-2} \ln \frac{L\theta_c}{r_1}$. The total number of contributing triplets, M_3 , can then be estimated by

$$M_3 \propto \int_{r_{min}}^{r_{max}} \frac{dN_1}{dr_1} \frac{1}{\theta_c^4} \ln \frac{L\theta_c}{r_1} dr_1 \quad (47)$$

where $\frac{dN_1}{dr_1}$ is the number of nodes with size between r_1 and $r_1 + \Delta r_1$ divided by Δr_1 in the limit that $\Delta r_1 \rightarrow 0$. Since $dN_1 \propto \frac{L^2}{\pi r_1^2}$ and $dr_1 \propto r_1$, we have

$$\frac{dN_1}{dr_1} \propto \frac{L^2}{\pi r_1^3}. \quad (48)$$

Therefore,

$$M_3 \propto \frac{L^2}{\pi \theta_c^4} \int_{r_{min}}^{r_{max}} \frac{1}{r_1^3} \ln \frac{L\theta_c}{r_1} dr_1 \quad (49)$$

$$= \frac{L^2}{2\pi \theta_c^4} \left[\frac{1}{2r_1^2} - \frac{1}{r_1^2} \ln \frac{L\theta_c}{r_1} \right]_{r_{min}}^{r_{max}}. \quad (50)$$

Substituting in $r_{min} \sim \sqrt{\frac{L^2}{\pi N}}$ and $r_{max} \sim L\theta_c$, we obtain

$$M_3 \propto \frac{L^2}{2\pi \theta_c^4} \left[\left(\frac{1}{2r_{max}^2} - \frac{1}{r_{max}^2} \ln \frac{L\theta_c}{r_{max}} \right) - \left(\frac{1}{2r_{min}^2} - \frac{1}{r_{min}^2} \ln \frac{L\theta_c}{r_{min}} \right) \right] \\ \sim \frac{L^2}{2\pi \theta_c^4} \left[\left(\frac{1}{2L^2\theta_c^2} \right) - \left(\frac{\pi N}{2L^2} - \frac{\pi N}{L^2} \ln \frac{L\theta_c}{\sqrt{L^2/\pi N}} \right) \right] \quad (51)$$

$$= \frac{N}{4\theta_c^4} \left[\left(\frac{1}{\pi\theta_c^2 N} \right) - 1 + 2 \ln (\theta_c \sqrt{\pi N}) \right] \quad (52)$$

$$= \frac{N}{4\theta_c^4} \left[\left(\frac{1}{\pi\theta_c^2 N} \right) - 1 + \ln \pi + \ln (\theta_c^2 N) \right] \quad (53)$$

$$\simeq \frac{N}{4\theta_c^4} \left[\left(\frac{1}{\pi\theta_c^2 N} \right) + 0.14 + \ln (\theta_c^2 N) \right]. \quad (54)$$

In the limit $\theta_c^2 N \gg 1$, we have $\frac{1}{\pi\theta_c^2 N} < \frac{1}{\theta_c^2 N} \ll 1$ and $\ln (\theta_c^2 N) \gg 1$. Hence,

$$M_3 \propto \frac{N}{\theta_c^4} \ln (\theta_c^2 N). \quad (55)$$

The cost of the computing the raw 3PCF is proportional to the number of contributing triplets. Hence, the computational cost of the raw 3PCF scales as $\frac{N}{\theta_c^4} \ln(\theta_c^2 N)$ for sufficiently large $\theta_c^2 N$. As $\theta_c^2 N \rightarrow \infty$, $\ln(\theta_c^2 N)$ can be considered as a constant since it increases only slowly. Hence, in this limit,

$$M_3 \propto \frac{N}{\theta_c^4}. \quad (56)$$

However, this convergence of the computational cost to $O(N\theta_c^{-4})$ behaviour as $\theta_c^2 N$ increases is very slow.

In the limiting case where $\theta_c \rightarrow 0$, the relation that the expected number of nodes in each annulus is proportional to θ_c^{-2} no longer holds. This is because $\theta_c^{-2} \rightarrow \infty$ while the number of non-overlapping nodes in the area remains bounded above by the total number of particles N . From the tree's perspective, subdivisions descend all the way down to the leaves for small θ_c , and perform full correlations among all triplets of particles, conforming to the intention of the subdivision process. On the other hand, as $N \rightarrow 0$ with a fixed θ_c , the subdivision procedure easily reaches the bottom of the tree due to the shallowness of the tree. Hence, the node-to-node correlations tend to be done at the leaf level for both small θ_c and small N . At the leaf level where p_1 contains a single galaxy, any pair of galaxies qualifies to form a contributing triplet with p_1 since, for the open angle criterion, the size of a single galaxy is extremely small compared to the space between galaxies. The possibility of finding a galaxy which qualifies to be a member of a contributing triplet containing p_1 is thus $N - 1$. In the limit where $\theta_c^2 N \ll 1$, the total number of triplets is $N(N - 1)(N - 2) \sim N^3$, so is the scaling of the computational cost for subdivisions and node-to-node correlations. Taking the limit as θ_c goes to 0, the θ_c -independent scaling of $O(N^3)$ is in agreement with the cost of the brute force approach.

Similarly, the 2PCF costs $O(N\theta_c^{-2})$ to compute. This is because the computation of the 2PCF involves M_2 triplets where

$$M_2 \propto \int_{r_{min}}^{r_{max}} \frac{dN}{dr} \frac{1}{\theta_c^2} dr \quad (57)$$

$$= \frac{L^2}{\pi\theta_c^2} \int_{r_{min}}^{r_{max}} \frac{1}{r^3} dr \quad (58)$$

$$= \frac{L^2}{2\pi\theta_c^2} \left(\frac{1}{r_{min}^2} - \frac{1}{r_{max}^2} \right) \quad (59)$$

$$= \frac{L^2}{2\pi\theta_c^2} \left(\frac{\pi N}{L^2} - \frac{1}{L^2\theta_c^2} \right) \quad (60)$$

$$= \frac{1}{2\pi\theta_c^4}(\pi\theta_c^2N - 1). \quad (61)$$

In the limit that $\theta_c^2N \gg 1$,

$$M_2 \propto \frac{N}{\theta_c^2}, \quad (62)$$

that is, the computational cost of the 2PCF scales as $N\theta_c^{-2}$.

The memory overhead of this new algorithm is $O(N)$ since the tree is stored in a 1D array of length $2N - 1$.

6.3 Tests of Computational Cost for 3PCF

As derived above, the computational cost of the raw 3PCF (after tree building) is expected to be $O(N\theta_c^{-4} \ln(\theta_c^2N))$ for $\theta_c^2N \gg 1$. Furthermore, for very large θ_c^2N , the scaling reduces to $O(N\theta_c^{-4})$.

The speed of the algorithm is tested for N up to 10^6 galaxies on CITA's 1.3GHz ItaniumII, Dell Poweredge 7250 computer. The set of computations for speed testing utilizes a randomly generated catalogue with the same attributes as the mock galaxy catalogue used for accuracy comparison. The catalogue is a list of galaxies with x, y coordinates, $\gamma_1, \gamma_2, \kappa$ and noise. Each of these attributes take random values between their minimum and maximum. While the coordinate components lie between 0 and 54000, γ_1, γ_2 and κ take values between -1 and 1 . To ensure numerical stability, the values of the noise is randomly selected in the range of $[1, 2)$. The 3PCF is computed for triplets with separations between 10 and $\sqrt{2} \times 54000$ with binning at logarithmic intervals of $2^{0.1}$. Here, we test and analyze the computing time of tree construction and that of the raw correlation function computation.

Figure 4 plots the total raw 3PCF computing time for the shear, κ and the weight as a function of the number of galaxies, N . Since the cost of tree building is independent of θ_c , the plot also shows the average tree building time over the different θ_c 's. In figure 4, we can see that the cost of the raw 3PCF computation dominates in the range of N considered. This shows that the cost of tree building has a much smaller prefactor than that of the raw correlation computation. In the following discussions about speed testing, we focus on the computation of raw correlation functions. The curves for the raw correlation computations appear to asymptotically approach the line with slope= 1 as N increases. However, the curves as shown are not quite $O(N)$ yet since the convergence of $\ln(\theta_c^2N)$ to a constant as θ_c^2N increases is slow. Only when θ_c^2N becomes quite a bit larger than those in the plot, would the behaviour

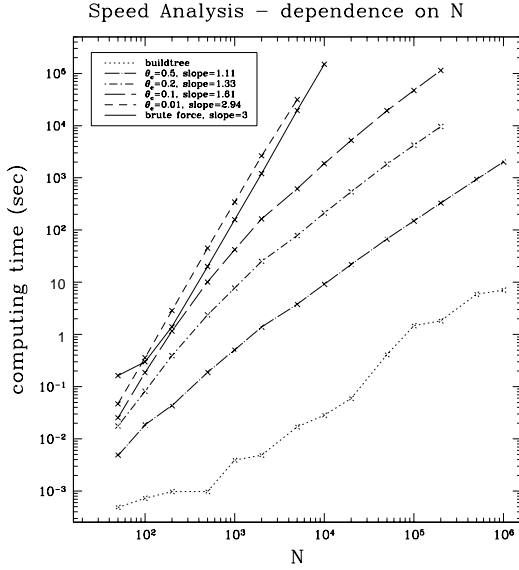


Fig. 4. A plot of the total raw 3PCF computing time for the shear, κ and the weight, against the number of particles. While the raw correlation functions for κ and for the weight are scalar, the shear raw correlation function consists of 8 components. The different lines correspond to different θ_c . The slopes given in the plot are measured at a fixed computing time of 1000 seconds. One expects the slope to approach 1 as $\theta_c^2 N \rightarrow \infty$. The plot also shows the average tree building time over the different θ_c 's.

of the curves exhibit linear quality. The slopes of the curves in figure 4 are all greater than one. However, it is evident from the figure that they decrease with increasing θ_c and N . This relation is further illustrated in figure 5.

Now, let us take a look at the dependence of the slope in figure 4 on the value of θ_c . We call this slope the scaling index. In figure 5, we plot the scaling index, which is measured at fixed N , as a function of θ_c . We observe that the scaling index decreases monotonically with θ_c for fixed N , and that it seems to approach 1 as $\theta_c \rightarrow \infty$. On the other hand, the scaling index also decreases monotonically with increasing N . These behaviours are consistent with our theoretical estimate that the dependence of the raw 3PCF computational cost on N tends to a linear relation as $\theta_c^2 N$ increases. We do not, in this work, study the detailed dependence of these scaling indices on θ_c and N .

In figure 6, we plot the total computing time for the raw correlation functions of the shear, κ , and the weight against the accuracy parameter θ_c while fixing N to be 5000. The curve flattens out in the small θ_c limit. This phenomenon is due to the extra factor of $\ln(\theta_c^2)$ in the computational cost as derived in section 6.2. However, as θ_c increases, the curve appears to asymptotically approach the line with slope = -4 . This is consistent with our expectation that the cost of computing the raw 3PCF scales as θ_c^{-4} for very high values of $\theta_c^2 N$, that is,

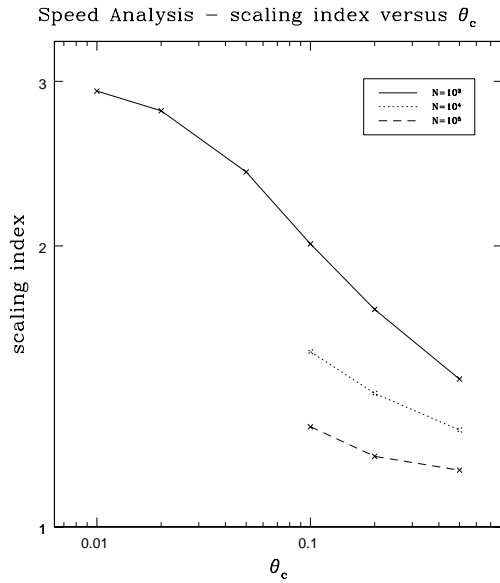


Fig. 5. A plot of the scaling index versus θ_c for different values of N . Here, the scaling index is defined to be the log-log slope of the computing time versus N . On each curve plotted here, the scaling indices are obtained by measuring the slopes in figure 4 at a fixed N . However, curves for $\theta_c = 0.02$ and 0.05 are not shown in figure 4 to avoid crowdedness.

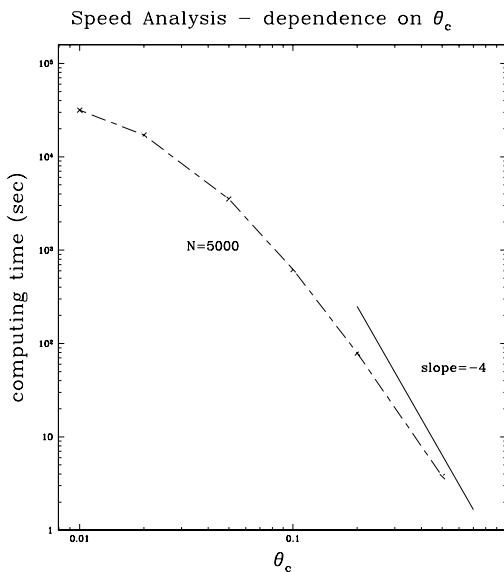


Fig. 6. A plot of the total raw 3PCF computing time for the shear, κ and the weight against θ_c for $N = 5000$. While the raw correlation functions for κ and for the weight are scalar, the shear raw correlation function consists of 8 components. A line with slope = -4 , which is expected to be the limit for large θ_c , is also plotted for the purpose of comparison.

when θ_c is sufficiently large for a fixed N .

6.4 Comparison of Computational Cost for 2PCF and 3PCF

Using our fast algorithm, the 2PCF in 2D costs $O(N(\log N)^2 + N\theta_c^{-2})$ to compute when $\theta_c^2 N \gg 1$. On the other hand, for sufficiently large $\theta_c^2 N$, the computing time of the 3PCF in 2D scales as $N(\log N)^2 + N\theta_c^{-4} \ln(\theta_c^2 N)$. The 3PCF scaling reduces to $O(N\theta_c^{-4})$ as $\theta_c^2 N \rightarrow \infty$. However, this convergence of the 3PCF computational cost to a linear relation in N is slow.

In comparison, using FFTs, the 2D two-point correlation function can be computed at the cost of $O(N \log N)$, and the three-point correlation functions at $O(N^2 + N\theta_c^{-2}(\log N)^2)$. The coefficient for FFTs can be very small, but the memory overhead of $O(N\theta_c^{-2} \log N)$ can be significant; and in highly clustered regimes, there is a significant inefficiency since the data must be gridded on the finest scale.

Moore et al. (2001) described an algorithm to compute the two-point function on a kd tree. They reported a scaling of $O(N^{3/2})$. The additional cost appears to arise because they loop over the correlation function bins and perform a gather operation on pairs, while our algorithm performs a scatter operation into the correlation function.

7 Conclusion

We have presented the framework to efficiently compute the n -point correlation function. This enables estimates of the full 3PCF in 2D for N as large as 10^6 . Historically, the computation of the 3PCF has been prohibitively expensive; the existing fast 2PCF algorithms often suffer loss of generality due to geometric limitations. In this work, we showed in detail how to compute the 2PCF and the 3PCF for a spin-2 field in the context of weak gravitational lensing. In 2D and for sufficiently large $\theta_c^2 N$, the 2PCF requires $O(N(\log N)^2 + N\theta_c^{-2})$ to compute while the 3PCF computation can be completed in $O(N(\log N)^2 + N\theta_c^{-4} \ln(\theta_c^2 N))$ time where θ_c is the critical open angle defined in section 3.1.2. Recall that the $O(N(\log N)^2)$ cost arises from the tree construction, and the remaining cost is due to subdivisions and node-to-node correlations. Since the raw correlation function computation is the prime consumer of computational effort in the range of consideration (see figure 4), the total computational cost at a fixed θ_c is dominated by $O(N)$ and $O(N \ln N)$ for the 2PCF and 3PCF respectively. As $\theta_c^2 N \rightarrow \infty$, the cost of computing the raw 3PCF tends to $O(N)$. On the other hand, when θ_c approaches zero,

one needs to descend all the way down to the leaves to accumulate the desired statistics. Therefore, the computational cost limits to $O(N^2)$ and $O(N^3)$ respectively for the 2PCF and 3PCF, similar to the cost of the brute force approach. We also generalized the algorithm to compute correlation functions of arbitrary order, with a discussion of its application to a scalar field in higher dimensional space.

The technique involves the construction of a balanced bisectional binary tree. The worst case error at each node is minimized by dividing perpendicular to the longest node extent. Bisection guarantees a tree of height no more than $\lceil 1 + \log_2 N \rceil$, and a memory requirement no more than $O(N)$.

At the same level of the tree hierarchy, all nodes are occupied by approximately the same number of particles; and all leaves contain exactly one particle. When walking the tree, we start from the 'root' node. Whenever the open angle criterion is fulfilled, we accumulate n -point statistics and terminate our pursuit along that path; otherwise, we move down the tree until the criterion is met by all n nodes or until we hit the leaves. Besides its speed, our tree method is favourable compared to the computation of the full 3PCF using FFT in that it is free of geometric restrictions and that it can be easily extended to compute correlation functions of arbitrary order.

For the upcoming lensing and CMB surveys such as the Canada-France-Hawaii-Telescope-Legacy-Survey, this rapid algorithm will allow an efficient analysis of the data in a tractable amount of computational effort.

We would like to thank Robin Humble for suggesting the algorithm, and Mike Jarvis for stimulating discussions. We are grateful to the referee for his valuable comments and useful suggestions.

References

- Barnes, J., Hut, P., Dec. 1986. *Nat*324, 446–449.
Barnes, J. E., Hut, P., Jun. 1989. *ApJ*70, 389–417.
Bentley, J. L., 1975. *Commun. ACM* 18 (9), 509–517.
Eriksen, H. K., Lilje, P. B., Banday, A. J., Gorski, K. M., Oct. 2003. *ArXiv Astrophysics e-prints*.
Gray, A. G., Moore, A. W., Nichol, R. C., Connolly, A. J., Genovese, C., Wasserman, L., Jan. 2004. *ArXiv Astrophysics e-prints*.
Jarvis, M., Bernstein, G., Jain, B., Jul. 2003. *ArXiv Astrophysics e-prints*.
Moore, A. W., Connolly, A. J., Genovese, C., Gray, A., Grone, L., Kanidoris, N., Nichol, R. C., Schneider, J., Szalay, A. S., Szapudi, I., Wasserman, L., 2001. In: *Mining the Sky*. pp. 71–+.
Padmanabhan, N., Seljak, U., Pen, U. L., 8 2003. *New Astronomy*, 581–603.

- Peebles, P. J. E., Oct. 1973. ApJ185, 413–440.
- Pen, U., Dec. 2003. MNRAS346, 619–626.
- Pen, U., Zhang, T., van Waerbeke, L., Mellier, Y., Zhang, P., Dubinski, J., Aug. 2003. ApJ592, 664–673.
- Sandvik, H. B., Magueijo, J., Aug. 2001. MNRAS325, 463–467.
- Santos, M. G., Balbi, A., Borrill, J., Ferreira, P. G., Hanany, S., Jaffe, A. H., Lee, A. T., Magueijo, J., Rabii, B., Richards, P. L., Smoot, G. F., Stompor, R., Winant, C. D., Wu, J. H., Jun. 2002. Physical Review Letters 88, 241302–+.
- Schneider, P., Lombardi, M., Jan. 2003. A&A397, 809–818.
- Totsuji, H., Kihara, T., 1969. PASJ21, 221–+.
- Verde, L., Heavens, A. F., Percival, W. J. et al., Sep. 2002. MNRAS335, 432–440.
- Wittman, D. M., Tyson, J. A., Kirkman, D., Dell’Antonio, I., Bernstein, G., May 2000. Nat405, 143–148.

A APPENDIX: Scheme of mainstream subdivision for n -PCF

The mainstream subdivision for the n -PCF is completed by the following operations:

```

j=0
Do i=1,n-1
  If (nodes(i)=nodes(i+1)) then
    j=j+1
  Else
    If (j>0) then
      Do k=0,j+1
        snodes=nodes
        snodes(i-j:i-j+k-1)=nodes(i-j).sub1
        snodes(i-j+k:i)=nodes(i-j).sub2
        call SUBDIVIDE(snodes,n,c=0)
      Enddo
    j=0
  Endif
Endif
Enddo.

```